Spectral gap induced by structural corrugation in armchair graphene nanoribbons

S. Costamagna, O. Hernandez and A. Dobry
Instituto de Física Rosario, Consejo Nacional de Investigaciones Científicas y Técnicas, Universidad Nacional de Rosario, Rosario, Argentina
(Dated: January 7, 2010)

We study the effects of the structural corrugation or rippling on the electronic properties of undoped armchair graphene nanoribbons (AGNR). First, reanalyzing the single corrugated graphene layer we find that the two inequivalent Dirac points (DP), move away one from the other. Otherwise, the Fermi velocity v_F decrease by increasing rippling. Regarding the AGNRs, whose metallic behavior depends on their width, we analyze in particular the case of the zero gap band-structure AGNRs. By solving the Dirac equation with the adequate boundary condition we show that due to the shifting of the DP a gap opens in the spectra. This gap scale with the square of the rate between the high and the wavelength of the deformation. We confirm this prediction by exact numerical solution of the finite width rippled AGNR. Moreover, we find that the quantum conductance, calculated by the non equilibrium Green's function technique vanish when the gap open. The main conclusion of our results is that a conductance gap should appear for all undoped corrugated AGNR independent of their width.

PACS numbers: 73.22.Pr, 73.23.Ad, 72.10.Fk

I. INTRODUCTION

The spectacular interest that have been raised from the recent isolation of an atomic Carbon layer, the graphene[1], is based on the unusual dynamics the electrons have in this material. In graphene, the electrons behaves as massless relativistic particles giving rise, for example, to a sequence of Hall plateau quite different than the one observed in 2D electrons systems confined in semiconductor heterojuntions. Also the transport properties are remarkable, the mobility of electrons in suspended graphene could be even higher than in any known semiconductor[2]. Even the existing of graphene as a two-dimensional atomic crystal and its stability under ambient conditions is an surprising fact. According to the Mermin-Wagner theorem, there is not should be long-range crystalline order in two dimensions at finite temperature. Even more, flexible membrane embedded in three-dimensional space should be crumpled because of long-wavelength bending fluctuations. However these fluctuations can be suppressed by anharmonic coupling between bending and stretching modes. As a result, single-crystalline membranes can exist but should be rippled[3]. Indeed, ripples were observed in graphene[4]. It has been proposed that they should play an important role in its electronic properties[5,6]. In particular, intrinsic rippling has been proposed as one of the possible mechanism for electron scattering to explain the variation of the resistivity with the number of charge carrier experimentally seen in graphene[7].

Between the research areas of graphene, a very important one is the study of nanoribbons where the sheets are catted with a particular pattern to manage the electrical properties. Depending on the type of the border edges they can be either in, namely, zigzag (ZGNR) or armchair configurations. It is known that a tight binding model predict that ZGNRs are always metallic while AGNRs can be either metallic or semiconductor, depending on their width[8]. However, experiments suggest that AGNR are always insulators with a gap that scale with the inverse of its width[9]. The effect of the corrugation on the electronic properties of graphene has been studied in previous works by a tight binding type model[10] and by ab-initio LDA calculation[11]. The rippling induce a nonuniform gauge field whose effects has been analyzed by analogy with an applied magnetic field. In this sens a pseudo Landau levels (LL) were predicted. Regarding nanoribbons the effects of the rippling on the conductivity were analyzed in a model which include also the effect of the disorder produced by charged impurities[12]. Although this approach is quite realistic it can not isolate only the effect of the rippling in order to known the contribution of each perturbation separately. Therefore, in this work, our mainly purpose is to analyze the effect of the corrugation on the electronic structure and the transport properties of AGNRs. First, as a necessary previous step we study the electronic properties of corrugated graphene layers. We reanalyze the condition for the appearance of a flat band associated with the zero LL. We show that an strong rippling on the sheet is necessary to produce such a flat band. Then, we focus on the armchair border type nanoribbons. Particularly we analyze the case of the zero gap band-structure AGNRs. We show that due to rippling an spectral gap is open in otherwise conducting ribbons. We subsequent analyze the quantum conductance by the non equilibrium green's function technique[13] (NEGF) and show that the opening of the gap manifest in a insulating behavior of the undoped samples.

The paper is organized as follows. In Section II we provide a detailed explanation of the corrugation model adopted and we study the effect of the corrugation on the electronic spectra of a graphene sheet. Then, in Section III we study the effect of the rippling on the electronic

spectra and the conduction properties of metallic AGNR. Finally, in Section IV we present the conclusions of our paper and we discuss it implicants.

II. THE EFFECT OF THE RIPPLING: THE GRAPHENE SHEET

Let us start by studying the effects of the corrugation on the electronic states for the case of 2D graphene layer. This question was examined in a series of previous papers[10,11]. As it will be the starting point of our study of a corrugated nanoribbons in the next Section, we reanalyze this problem in the present Section. This will be presented after a detailed description of the model adopted.

A. The model

We describe the electronic properties of graphene layer by means of a tight-binding model with one π-orbital for each Carbon atom and nearest-neighbor hopping between them. Carbon atoms arrange in a honeycomb lattice. It is not a Bravais lattice but can be constructed from the hexagonal lattice by putting a basis of two atoms. The hexagonal lattice could be constructed as $\mathbf{R^l} = l_x\mathbf{a}_1 + l_y\mathbf{a}_2$ with l_x and l_y integers, $\mathbf{a}_1 = \frac{a}{2}(3,\sqrt{3})$ and $\mathbf{a}_2 = \frac{a}{2}(3,-\sqrt{3})$ are the primitive vectors. The basis is given by the atom A sited at $\mathbf{R^l}$ and B at $\mathbf{R^l} + \frac{a}{2}(1,\sqrt{3})$. $a \sim 1.41\mathring{A}$ is the lattice constant and hereafter will be taken as unit of distances.

The corrugation was included as a sinusoidal function which module the z coordinate of each lattice site. The x and y coordinates remain into its values in the honeycomb lattice. For simplicity, we assume that rippling only depend on the x direction (see fig. 1 for the case of a nanoribbon). Then, the adopted $z(x)$ function reads:

$$z(x) = h_0 sin\left(\frac{2\pi}{\tau}x\right) \qquad (1)$$

where h_0 is the amplitude and τ the period of the rippling. This simple model for the corrugation has been used in previous works[10,11]. As a superposition of functions of the type (1) with different wave vectors and different amplitudes could generate a quite general corrugation, our study should be taken as a starting point for the effect of a general corrugated function. Evermore as we point to the study of nanoribbons which by definition are much longer than wider the one-dimensional character of the rippling function is justified.

The modulated structure induce an spacial variation of the hopping parameter t, being now dependent on the distance between the atoms. Developing t up to first order in the perturbed distance between the nearest neighbor (Δa) we have:

$$\begin{aligned} t &= t_0 + \frac{t_0}{a}\alpha\Delta a \\ \Delta a &= \sqrt{a + (z(x) - z(x'))^2} - a \end{aligned} \qquad (2)$$

where $t_0 \approx 2.66eV$ is the hopping parameter of the undeformed graphene which is taken as a unit of energy in the present work. $\alpha = \frac{\partial \log t}{\partial \log a} \sim 2$, whose value is taken from Ref. (2). The rippling also produce a bending of the p-orbitals. However it has been shown that the relative change of the hopping due to the bending is weaker than the one due to the change of the bond length[12]. For simplicity, we neglect this effect in the present paper.

The tight binding Hamiltonian in the presence of the corrugation becomes:

$$H = -\sum_{\boldsymbol{l},\boldsymbol{\delta},\sigma} t[z_{B\boldsymbol{l}+\boldsymbol{\delta}} - z_{A\boldsymbol{l}}](c^\dagger_{\boldsymbol{l}A,\sigma}c_{\boldsymbol{l}+\boldsymbol{\delta}B,\sigma} + h.c.) \qquad (3)$$

where $\boldsymbol{l} = (l_x, l_y)$ denotes the integer coordinates in the hexagonal Bravais lattice and $\boldsymbol{\delta} = \{(0,0),(-1,0),(-1,1)\}$.

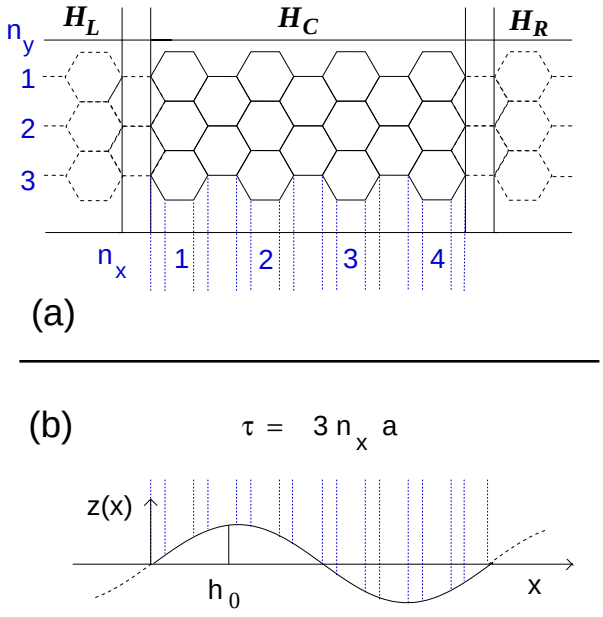

FIG. 1: (a) Schematic view of an armchair graphene nanoribbon. Vertical lines separates the regions adopted for the conductance calculation described in Sec.III B trough the Hamiltonians displayed on top. The central region possesses $n_x = 4$ and $n_y = 3$, listed as indicated. (b) Side view in the $x-z$ plane of the displacement of Carbon atoms due to rippling. h_0 is the amplitude and τ the period. a is the lattice constant of graphene. Vertical dotted lines from (a) to (b) gives reference for the actual positions of Carbon atoms in the corrugated nanoribbon.

B. Dirac equation

A low energy Hamiltonian could be obtained from (3) expanding the Fourier transform of the electron operators around two of the inequivalent points where the dispersion relation vanish, namely the Dirac points (DP). We choose these points as given by $\mathbf{K} = \frac{2\pi}{3a}(1, \frac{1}{\sqrt{3}})$ and $\mathbf{K}' = \frac{2\pi}{3a}(1, -\frac{1}{\sqrt{3}})$. In addition we assume a smooth variation of $z(x)$, i.e. $\tau >> a$. The low energy physics is described by the sum of two Dirac Hamiltonians for massless particles in a pseudo-magnetic field. It is given by:

$$\begin{aligned} H &= v_F \int dr^2 (\mathbf{\Psi}_1^\dagger(r)\boldsymbol{\sigma}^* \cdot (-i\boldsymbol{\nabla} + \boldsymbol{A}(r))\mathbf{\Psi}_1(r) \\ &+ \mathbf{\Psi}_2^\dagger(r)\boldsymbol{\sigma} \cdot (-i\boldsymbol{\nabla} - \boldsymbol{A}(r))\mathbf{\Psi}_2(r)) \end{aligned} \quad (4)$$

where $v_F = \frac{3t_0 a}{2}$ is the Fermi velocity, $\boldsymbol{\sigma} = (\sigma_x, \sigma_y)$ is the vector of the Pauli matrices and $\boldsymbol{\sigma}*$ its complex conjugate. The two component field is $\mathbf{\Psi}_i = (c_{iA}, c_{iB})$ with $c_{i,A(B)}$ creation field operator over the A(B) sublattice The index $i = 1, 2$ refers to states with momentum near $\mathbf{K}$, $\mathbf{K}'$. The gauge vector $\boldsymbol{A}(r) = (A_x, A_y)$ were induced by the rippling and is given by:

$$\begin{aligned} A_x &= 0 \\ A_y &= -\frac{\alpha}{4}(\partial_x h)^2 = -\frac{\alpha}{4}(h_0 q)^2 (cos\Big(\frac{4\pi}{\tau}x\Big) + \frac{1}{2}) \\ &\equiv \hat{A}_y + k_0 \end{aligned} \quad (5)$$

$k_0 = -\frac{\alpha}{8}(h_0 q)^2$ is the $k = 0$ Fourier component of A_y and $q = \frac{2\pi}{\tau}$ the wave vector of the rippling. Note that as the time reversal symmetry is not broken by the rippling, this implies that the coupling of $\mathbf{\Psi}_1$ with $\boldsymbol{A}(r)$ have different sign than the one of $\mathbf{\Psi}_2$. This fact will be important in the study of the nanoribbons undertaken in the next Section.

The Dirac equation in a magnetic field corresponding to the one particle problem generated by eq. (4) at $i = 1$ could be exactly solved for the zero energy eigenstate. By following similar steps as in Ref. 14 we find the following two degenerated eigenfunctions:

$$\begin{aligned} \Psi_{+0}(x, y) &= \frac{N}{\sqrt{L_y L_x}} e^{-ik_0 y} \begin{pmatrix} e^{F(x)} \\ 0 \end{pmatrix} \\ \Psi_{-0}(x, y) &= \frac{N}{\sqrt{L_y L_x}} e^{-ik_0 y} \begin{pmatrix} 0 \\ e^{-F(x)} \end{pmatrix} \end{aligned} \quad (6)$$

with $F(x) = \frac{\alpha}{8} h_0^2 q \sin(2qx)$ and $L_{x,y}$ the system length in both direction. N is a normalization constant given by $N = [I_0(\frac{\alpha h_0^2 q}{4})]^{-\frac{1}{2}}$ with I_0 the modified Bessel function of zero order.

The low energy eigenstates of (4) can be studied by degenerated perturbation theory over the zero energy states $\Psi_{+0}(x, y)$ and $\Psi_{-0}(x, y)$. The potential A_y is periodic with period $\frac{\tau}{2}$. Therefore the solutions of (4) fulfill the Bloch theorem. They will have the form:

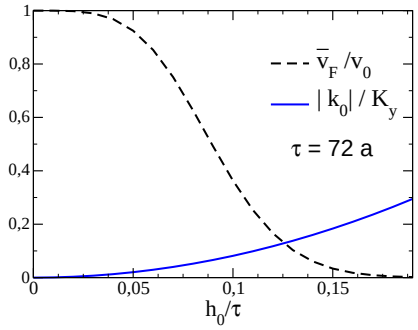

FIG. 2: Shifting of the DP $|k_0|$ normalized to the y coordinates of this point (K_y) as a function of h_0/τ (solid line). We also shown $\frac{\bar{v}_F}{v_F}$ giving the reduction of the Fermi velocity (dotted line).

$$\Psi_{n,\boldsymbol{k}}(x, y) = e^{i\boldsymbol{k}\cdot\boldsymbol{r}} \psi_{n,k_x}(x) \quad (7)$$

where n is a band index and k_x belong to the Brillouin zone of the imposed periodic lattice i.e. $-\frac{2\pi}{\tau} \leq k_x < \frac{2\pi}{\tau}$. Otherwise there is not restrictions on the values of k_y. Note that (6) is of the form of (7) with a quasi-momenta of the zero energy eigenstates given by $\boldsymbol{k_0} = (0, -k_0)$. and function $\psi_{0,k_x}(x)$ given by:

$$\psi_{0,\boldsymbol{k}}(x) = \frac{N}{\sqrt{L_y L_x}} \begin{pmatrix} a_0 e^{F(x)} \\ b_0 e^{-F(x)} \end{pmatrix} \quad (8)$$

a_0 and b_0 satisfying $\sqrt{a_0^2 + b_0^2} = 1$. In (7) the Bloch function fulfill $\psi_{n,k_x}(x + \frac{\tau}{2}) = \psi_{n,k_x}(x)$ and satisfy $H(\boldsymbol{k})\psi_{n,\boldsymbol{k}} = E_{n,\boldsymbol{k}}\psi_{n,\boldsymbol{k}}$, with $H(\boldsymbol{k})$ given by:

$$\begin{aligned} H(\boldsymbol{k}) &= H_0(\boldsymbol{k}) + H_{int}(\boldsymbol{k}) \\ H_0(\boldsymbol{k}) &= v_F \boldsymbol{\sigma}^* \cdot (-i\boldsymbol{\nabla} + \hat{\boldsymbol{A}}(\boldsymbol{r})) \\ H_{int}(\boldsymbol{k}) &= v_F \boldsymbol{\sigma}^* \cdot (\boldsymbol{k} + \boldsymbol{k_0}) \end{aligned} \quad (9)$$

As $H_0(\boldsymbol{k})\psi_{0,\boldsymbol{k}}(x) = 0$ we identify $H_0(\boldsymbol{k})$ as the unperturbed Hamiltonian. The approximated near-zero energy eigenstates could be obtained by diagonalizing H_{int} in the subspace of the degenerated zero energy states. H_{int} proyected onto this subspace is a 2×2 matrix called $\boldsymbol{h}$ and given by:

$$\begin{aligned} \boldsymbol{h} &= \hat{v}_F \begin{pmatrix} 0 & k_x + i(k_y + k_0) \\ k_x - i(k_y + k_0) & 0 \end{pmatrix} = \\ &= \hat{v}_F \boldsymbol{\sigma}^* \cdot (\boldsymbol{k} + \boldsymbol{k_0}) \end{aligned} \quad (10)$$

$\hat{v}_F = N^2 v_F$ is a renormalized Fermi velocity. The eigenvalues of (10) are:

$$E_1(k_x, k_y) = \pm \hat{v}_F \sqrt{k_x^2 + (k_y + k_0)^2} \quad (11)$$

We see that the main effects of the corrugation are:

1. DP sited in $\boldsymbol{K}$ have been shifted to $\boldsymbol{K} - \boldsymbol{k_0}$.

2. $\hat{v}_F$ decrease by increasing rippling.

If we had studied the behavior near $\mathbf{K}'$ by analyzing the second term in (4) we would have obtained instead of eq. (11) the result:

$$E_2(k_x, k_y) = \pm\hat{v}_F\sqrt{k_x^2 + (k_y - k_0)^2} \tag{12}$$

Therefore $\boldsymbol{K'}$ moves opposite than $\boldsymbol{K}$. As k_0 is a negative quantity the two DP away each other in presence of the rippling. In Fig. 2 we show the relationship $\frac{|k_0|}{K_y}$ and $\frac{\hat{v}_F}{v_F}$ as a function of $\frac{h_0}{\tau}$

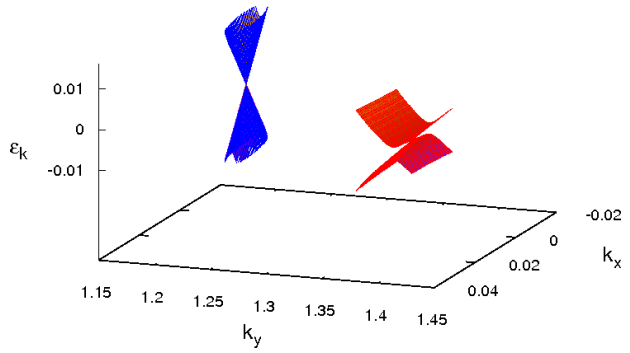

FIG. 3: Low energy band structure of uncorrugated (blue) and corrugated (red) graphene layers. The corrugation parameters are $\tau = 72\ a$ and h_0 equals 0.0, which correspond to the Dirac cone, and 6.0 in units of a, respectively. This result qualitatively agree with the obtained by means the Dirac equation including the pseudo-magnetic field.

For completeness, let us provide a comparison, just at a qualitative level, of the above findings with the band structure of corrugated graphene layers. Since we are trying to detect the displacement of the Dirac points, first we must compute the band structure of the uncorrugated case. Note here that since the adopted ripple develops in the x axis direction with a period equal to τ, as can be seen in fig.1 (b), then the unit cell must be extended up to include the whole rippled region from where the hopping becomes repeated again. This enlargement of the unit cell produces thus a reduction of the k_x components of the Dirac points K and K' due to band reflexion at the border of the original first Brilloun zone. As can be seen in the fig.3, where we show the low energy spectrum obtained for corrugations whose period is $\tau = 72\ a$ and with amplitudes h_0 0.0 and 6.0 in units of a, the corrugation effectively shifts the Dirac point, located originally at K, in the k_y direction. Also, in addition to this shift and in accord with the earlier predictions, the observed small slope of the dispersion bands of corrugated graphene implies a lower Fermi velocity of electrons near the Fermi level. It should be mention here that this result is related with the appearance of Landau like levels (LL) induced by rippling and studied in related works[10]. Note that from Fig. 2 we see that large values of $\frac{h_0}{\tau}$ are required to obtain a total flattening of the band. This could be interpreted as that the predicted zero LL appears only when the rippling is strong enough. This conclusion is consistent with the results of Ref. 11. In this work it was shown that as a result of the relaxation of the structure, the corrugation decrease and the flat band disappears from the spectra.

III. THE EFFECT OF THE RIPPLING: ARMCHAIR GRAPHENE NANORIBBONS

Let us now turn into the main subject of this work which is the study of the effects of corrugations on the spectra of graphene nanoribbons. As we have mentioned in the Introduction, a tight binding based description of the electronic properties of the ribbons predict that, depending on their width and border edge type, they can be metallic, with zero band gap, or insulators[8]. For example, for armchair edge (fig.1) there are specific values of the width has for which metallic behavior is expected. Otherwise they should be insulators. In spite of that, the experiments shown that graphene nanoribbons are insulators independent of their width[9]. Though device fabrication process does not give atomically precise control on the type of edges, this seems to show that a pure tight binding model is not enough to describe the GNR as it is for the sheets. Both, electronic correlation[15] and edge disorder[16,17], have been proposed as possibles mechanisms that give rise to this behavior. In this Section we show that rippling could give an additional source for the electronic gap, at least for the armchair edge type.

A. Dirac equation with boundary conditions

As for the infinite graphene sheet, it is possible to study the low energy electronic structure of graphene nanoribbons by a Dirac like equation, but in this case adequate boundary conditions must be imposed[8]. For armchair edges, the valley states near the DPs, $\mathbf{K}$ and $\mathbf{K}'$, get admixture and metallic behaviors are obtained for certain widths. We have described in the previous Section that the rippling produce a shift of the two inequivalent DPs. As we will shown below, to include only this shifting is enough to obtain a drastic change in the electronic behavior of AGNRs due to corrugations.

The wavefunction for sub-lattices A (B) are therefore given by:

$$\begin{aligned}\Phi_{A(B)}(\boldsymbol{r}) &= e^{i(\boldsymbol{K}-\boldsymbol{k_0})\cdot\boldsymbol{r}}\Psi_{1,A(B)}(\boldsymbol{r}) \\ &+ e^{i(\boldsymbol{K'}+\boldsymbol{k_0})\cdot\boldsymbol{r}}\Psi_{2,A(B)}(\boldsymbol{r})\end{aligned} \tag{13}$$

where $\Psi_{1,A(B)}$ are the components of the spinor wave function for states near $\boldsymbol{K}$ and $\Psi_{2,A(B)}$ the ones near $\boldsymbol{K'}$. For AGNR the wave function should vanish at $y = 0$ and $y = L_y$.

If we neglect other effect than the shifting of the DP, the translational symmetry is preserved and implies that $\Psi_{1(2),A(B)}(\boldsymbol{r})$ could be written as:

$$\Psi_{1(2),A(B)}(\boldsymbol{r}) = e^{ik_x x}\phi_{1(2),A(B)}(y) \quad (14)$$

The solutions of the Dirac equation with the previous stated boundary conditions (BC) has now the form:

$$\begin{aligned}\phi_{1,B} &= e^{ik_n y} \\ \phi_{2,B} &= -e^{-ik_n y},\end{aligned} \quad (15)$$

with the energies given by:

$$\epsilon = \pm v_F\sqrt{k_x^2 + k_n^2}. \quad (16)$$

The values of k_n fulfills $\sin[(k_n + K_y - k_0)L_y] = 0$ and are given by:

$$k_n = \frac{n\pi}{L_y} - K_y + k_0 \quad (17)$$

In absence of k_0, k_n could vanish giving rise to a gapless spectra as is seen from Eq. (16). This is the case when the width of the ribbons is $L_y = 3(n_y - 1)\sqrt{3}a$ with n_y integer. However when k_0 is present the condition for gapless spectra could not be fulfilled in general. Even more for the L_y and n_y giving a gapless spectra in absence of the rippling we now have a dispersion of the form $\epsilon = \pm v_F\sqrt{k_x^2 + k_0^2}$ and therefore a gap given by:

$$\Delta = 2v_F k_0 \sim \left(\frac{h_0}{\tau}\right)^2 \quad (18)$$

Thus, from the previous consideration we expect a gap for AGNR due to rippling that scale as $\left(\frac{h_0}{\tau}\right)^2$. A more accurate treatment of the rippling will correct the constant multiplying the scaling law and possible produce correction to this scaling for large enough rippling values.

To confirm the previous predictions we have calculated numerically the eigenstates of corrugated armchair graphene nanoribbons. This was performed following the steps described at the end of Sec. II taken into account here the armchair ribbon geometry displayed on fig. 1. As we were interested in detecting the gap and in analyzing its dependence with the corrugation, we have explored a wide set of rippling parameters keeping fixed the width of the ribbons in the values in which they possesses metallic behavior being uncorrugated. Figure 4 shows the zero energy gap as a function of h_0/τ for the various sets of parameters displayed on the plot, for a width given by $n_y = 8$. Note that for the small values of h_0/τ included in this figure, the gap does not depend on h_0 and τ independently but on the ratio between these quantities. We have fitted the calculated gap using the least squares method for a function of the type $\Delta = C(\frac{h_0}{\tau})^2$ obtaining excellent agreement with correlation coefficients near one with a precision of 10^{-3}. The obtained fitting is shown in Fig. 4 with dotted line. In accord to the stated above results, we have observed that by including higher values of h_0/τ the fitting become less precise.

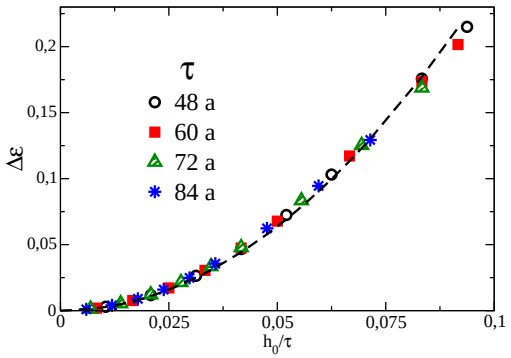

FIG. 4: Quadratic behaviour of the zero energy gap as a function of h_0/τ in corrugated armchair graphene nanoribbons. Values obtained from band structure calculations for the different corrugation parameters sets displayed on the plot. The dotted-line is a fitting to a quadratic law (see text for details).

B. Quantum Conductance

Finally, we analyze how all the above findings affect the electronic transport properties of the armchair graphene nanoribbons. For this purpose, we employed the non-equilibrium Green's function formalism[13,15] which provides an useful method to study the quantum conductance in nanoscopic systems.

Before a discussion of the results let us present a briefly description of the method and the implementation adopted. We considered one corrugated unit cell, as central region H_C, connected to two semi-infinite outstanding graphene nanoribbons flat leads, all having width length $n_y = 8$ which corresponds to a zero band gap structure in the uncorrugated case. The hopping parameter in both leads Hamiltonians, H_L and H_R, being flat, is t_0. Hence, the whole system is then described by

$$H = H_C + H_R + H_L + h_{LC} + h_{LR}, \quad (19)$$

where h_{LC} and h_{LR} are the hopping terms from both leads to the central corrugated portion of nanoribbon, which we set equal to t_0 (see fig.1(a)). Within this formalism, the Landauer conductance $G(E)$ of the system, in a zero bias approximation, is expressed as

$$G(E) = \frac{2e^2}{h}T(E) \quad (20)$$

where $T(E)$ is the transmission function given by $T(E) = \mathrm{Tr}(\Gamma_L(E)\mathcal{G}_C(E)\Gamma_R(E)\mathcal{G}_C^\dagger(E))$, with $\Gamma_\ell = -2\mathcal{I}m(\Sigma_\ell(E))$ ($\ell = L, R$) being the couplings of the corrugated graphene nanoribbon to the leads, and $\mathcal{G}_C(E) = (E - H_C - \Sigma_L - \Sigma_R)^{-1}$ the total Green's function including the leads self energies, Σ_L and Σ_R. These self energies must be calculated through the leads surfaces Green functions (SGF). Although it was reported a very time efficient way to compute the SGF of graphene nanoribbons leads (See Fig. 2 of Ref. 18), for the sake of simplicity we implemented the recursive iteration procedure, given by $g_\ell = (E - H_\ell - T_\ell^\dagger g_\ell T_\ell)^{-1}$, where H_ℓ is the unit cell lead Hamiltonian and T_ℓ is the interlayer coupling in the semi-infinite lead. For the small width nanoribbons studied here we have checked that a fast convergence is obtained. In the iterative procedure, we set the tolerance as 10^{-6}.

Figures 5 (a), (b) and (c), show the transmission coefficients obtained for armchair border type nanoribbons whose period τ is 72 a and with amplitudes $h_0 = 0.0, 3.0$ and 6.0 in units of a, respectively. In the left panels of the plots we included the corresponding low energy bands structure computed numerically following the description given at the end of Section II suited for the nanoribbon case. The band reflexion at the first Brillouin zone can clearly be seen in fig. 5 (a) which correspond to the uncorrugated case. Here, and such as is expectable, the transmission coefficient is equals to one at the Fermi energy. In the fig. 5 (b) the band gap at the Fermi energy appears, and accordingly to this the transmission becomes reduced. The fact that it do not reach zero is produced because the central region possesses only one corrugated unit cell. Increasing the amplitude of the rippling the gap becomes broader as is observed in fig. 5 (c) and the transmission goes to zero around the Fermi energy. These results are consistent with the obtained above by solving the Dirac equation. Here also, a second null conductance region appears above a thin perfect conductance interval at higher energies. In addition to these results, obtained keeping fixed τ_x and varying h_0, we calculated $T(E)$ for a wide range of corrugation periods and amplitudes, finding in all cases the appearance of a gap at low energies around E_F.

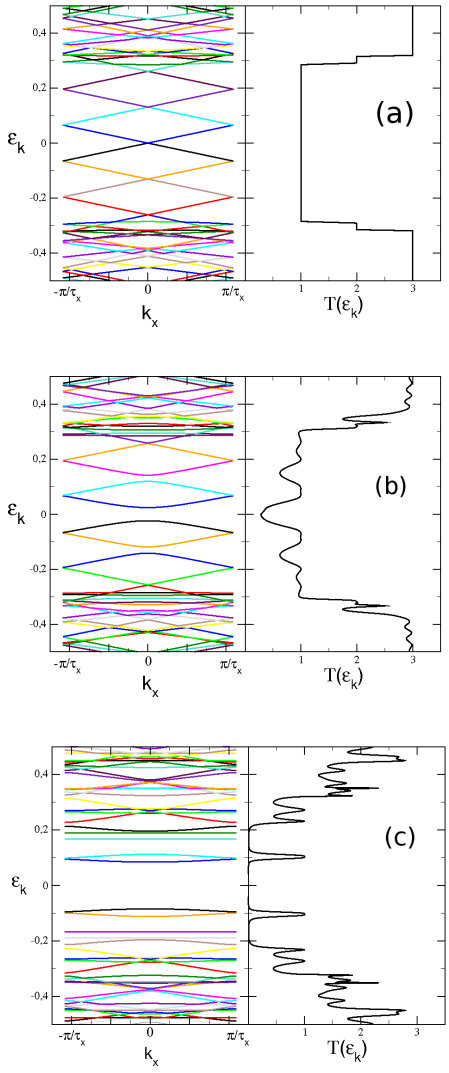

FIG. 5: Transmission coefficient of corrugated armchair graphene nanoribbons. $n_x = 24$, $n_y = 8$ and $h_0 = 0$ (a), $h_0 = 3$ (b) and $h_0 = 6$ (c), in units of a . In each left panel we included the corresponding low energy band structure which serve to a better analysis of the behavior of $T(E)$.

IV. CONCLUSIONS

After having analyzed the Dirac equation including the pseudo-magnetic field induced by the corrugation, and having explored numerically a wide realistic range of rippling parameters sets, we have found that the corrugations produces a gap in the low energy electronic spectrum of otherwise conducting armchair graphene nanoribbons. We have found that this gap scale quadratic with the rate between the high and the wavelength of the deformation. Accordingly to this, the quantum conductance $G(E)$ of the ribbons, calculated by the NEGF formalism, vanish around the Fermi energy of undoped corrugated samples.

These results was preceded by an analysis of the corrugation effects over the electronic spectra of graphene layers. Therein, we have found that the corrugation just shift the Dirac points and renormalizes the Fermi velocity. These findings agree with the results of numerical calculations.

In view of this, we conclude that the corrugations are an important source of gap in the spectra in addition to the electronic correlations to which typically is assigned this effect[15]. Although our study was performed modeling the corrugations by single sinusoidal functions, since any lattice deformation could be approximated quite well by an adequate sum of sins, we strongly believe that the results obtained here are extensible to general cor-

rugations. Moreover, our findings could be revealed in future experiments undertaken on the suspended clean sampled[19] where extrinsic effect would be minimized. For these reasons we expect that our paper motivates experimental works to determine the dependence of the gap with the corrugation parameters that can be varied by changing the applied stress[20,21] or the temperature.

Acknowledgments

This work was supported in part by grant PICT 1647 (ANPCYT).

[1] K. S. Novoselov, A. K. Geim,S. V. Morozov,D. Jiang, Y. Zhang, S. V. Dubonos, I. V. Grigorieva, A. A. Firsov , Science **306**, 666 (2004).
[2] A. H. Castro Neto, F. Guinea, N. M. R. Peres, K. S. Novoselov and A. K. Geim, Rev. Mod. Phys. **81**, 109-161 (2009).
[3] M. J. Bowick, A. Travesset, Phys. Rep., **344**, 255 (2001).
[4] J. C. Meyer, A. K. Geim, M. I. Katsnelson, K. S. Novoselov, T. J. Booth and S. Roth, Nature **446**, 60-63 (2007).
[5] S. V. Morozov, K. S. Novoselov, M. I. Katsnelson, F. Schedin, L. A. Ponomarenko, D. Jiang, and A. K. Geim, Phys. Rev. Lett. **97**, 016801 (2006).
[6] E. Kim and A. H. Castro Neto, EPL **84**, 57007 (2008).
[7] M.I Katsnelson and A.K Geim, Phil. Trans. R. Soc. A **366** 195 (2008).
[8] L. Brey and H.A. Fertig, Phys. Rev. B **73**, 235411 (2006).
[9] M. Y. Han, B. Ozyilmaz, Y. Zhang, and P. Kim Phys. Rev. Lett. **98**, 206805 (2007).
[10] F. Guinea, M. I. Katsnelson, M. A. H. Vozmediano, Phys. Rev. B **77**, 075422 (2008).
[11] T. O. Wehling, A. V. Balatsky, A. M. Tsvelik, M. I. Katnelson and A. I. Lichtenstein, EPL **84**, 17003 (2008).
[12] J. W. Klos, A. A. Shylau, I. V. Zozoulenko, Hengyi Xu, T. Heinzel, arXiv.09084228v2 (2009).
[13] Electronic Transport in Mesoscopic Systems, S. Datta, Cambridge University Press, 1995, Paperback Edition 1997.
[14] I. Snyman, Phys. Rev. B **80** 054303 (2009).
[15] H. Santos, L. Chico, and L. Brey, Phys. Rev. Lett. **103**, 086801 (2009).
[16] T. C. Li, and Shao-Ping Lu, Phys. Rev. B **77**, 085408 (2008).
[17] E. R. Mucciolo, A. H. Castro Neto, and C. H. Lewenkopf, Phys. Rev. B **79**, 075407 (2009).
[18] R. Golizadeh-Mojarad, A.N. M. Zainuddin, G. Klimeck and S. Datta, Journal of Comp. Electronics **7**, Vol. 3, 407-410 (2008).
[19] K. I. Bolotin, K. J. Sikes, J. Hone, H. L. Stormer, and P. Kim , Phys. Rev. Lett. **101**, 096802 (2008)
[20] E. Prada, P. San-Jose, G. Len, M. M. Fogler and F. Guinea, arXiv:0906.5267v2.
[21] V. M. Pereira, A. H. Castro Neto and N. M. R. Peres, Phys. Rev. B **80**, 045401 (2009).